A methodology for the low-cost optimisation of small wind turbine performance

A. Arroyo*, M. Manana, C. Gomez, I. Fernandez, F. Delgado, Ahmed F. Zobaa

University of Cantabria. Department of Electrical and Energy Engineering
Av. Los Castros s/n. 39005. Santander, Spain

Abstract

The increasing use of small wind energy has made it necessary to develop new methods to improve the efficiency of this technology. This improvement is best achieved considering the interaction between the various components, such as the wind rotors, the electrical generators, the rectifiers and the inverters, as opposed to studying the individual components in isolation. This paper describes a methodology to increase the efficiency of Small Wind Turbines (SWTs) equipped with a Permanent Magnet Synchronous Machine (PMSM). To achieve this objective, capacitor banks will be connected between the PMSM and the rectifier. This methodology is motivated by two clear aims. The first one is to operate the SWT with its maximum power coefficient C_p. The second one is to select the most suitable capacitor bank for each wind speed to optimise the energy supplied to the grid. The methodology will be tested on a commercial 3.5 kW SWT, and the results will be studied to determine its feasibility.

*Corresponding author. Tel.: +34-942201371; fax: +34-942201385.
E-mail address: arroyoa@unican.es (A. Arroyo)

Keywords: Capacitor, Wind power generation, Performance optimisation.

GLOSSARY

Figure glossary

1. INTRODUCTION

The small wind industry is experiencing significant growth and is becoming increasingly competitive. Currently, robust equipment that maximises energy production and minimises manufacturing costs is being sought.

Some studies to achieve these objectives have focused on:

- Improving the energy storage system [1],
- Designing new Permanent Magnet Synchronous Machines (PMSMs) [2],
- Improving the aerodynamic design of Small Wind Turbines (SWTs) [3, 4],
- Controlling the pitch angle [5],
- Enhancing the inverter operation [6].

Previous works have used capacitors behind the rectifier to create a Power Factor Control (PFC) and to improve the SWT efficiency [7, 8, 9].

This paper presents a methodology to optimise the efficiency of SWTs based on a PMSM. To test this methodology, it is necessary to create a model of the whole system. The Simulink software package was used for this purpose [10]. To optimise the system, two aspects are considered:

1. The aerodynamic factor: the Maximum Power Point Tracker (MPPT) [11] is calculated to extract the maximum energy from the wind [12]. Using the MPPT and the SWT operating surfaces (obtained by means of the Simulink model), the optimal relationship between the continuous voltage of the rectifier v_{dc} and the grid power P_{grid} can be determined. This relationship must be set in the inverter, and it is known as the Maximum Power Characteristic Curve (MPCC).
2. The capacitor bank effect: when a capacitor bank is connected, the armature reaction produces a magnetising effect in the PMSM that is added to the magnetic field generated by the magnets. As a result, a higher voltage at the machine terminals is generated [13, 14].

This methodology will be tested in a commercial 3.5 kW SWT with a PMSM, and the system improvements will be verified. Finally, an economic study will be conducted, in which the well-known Weibull Distribution (WD) will be employed [15].

2. SYSTEM MODEL

A system model is necessary to use the methodology presented here, and Simulink was used for this purpose [10]. This model makes it possible to analyse the SWT in detail and to evaluate its performance under various operating conditions.

First, a PMSM model must be created with the intention of including it in the system model. This model was constructed using the electrical equations

of synchronous machines. Eq. (1) defines the flux at the stator of the PMSM:

$$\begin{aligned}\psi_{ea}(t) =&(L_{\sigma_e} + M_{aa})i_{ea}(t) + M_{ea}i_{eb}(t) + M_{ea}i_{ec}(t)+ \\ &+ \psi_f cos(\theta_e(t))\end{aligned} \tag{1}$$

where

$\psi_{ea}(t)$	Total instantaneous flux in the stator phase "a",
L_{σ_e}	Leakage inductance of a stator phase,
M_{aa}	Inductance due to the magnetisation flux generated by the phase "a" on itself,
M_{ea}	Inductance due to the magnetisation flux generated by the other phases on the phase "a",
ψ_f	Flux generated by the rotor,
$\theta_e(t)$	Electrical angle between the rotor and the stator,
$i_{ea}(t), i_{eb}(t), i_{ec}(t)$	Instantaneous current flowing through the stator phases.

if $i_{ea}(t) = -(i_{eb}(t) + i_{ec}(t))$, then:

$$\psi_{ea}(t) =(L_{\sigma_e} + M_{aa} - M_{ea})i_{ea}(t) + \psi_f cos(\theta_e(t)) \tag{2}$$

Given the geometry of the stator phases,

$$M_{ea} = M_{aa}cos(\frac{2\pi}{3}) = -\frac{M_{aa}}{2} \tag{3}$$

and incorporating it into Eq. (2),

$$\psi_{ea}(t) = (L_{\sigma_e} + \frac{3M_{aa}}{2})i_{ea}(t) + \psi_f cos(\theta_e(t)) \tag{4}$$

the total flux at phase "a" can be expressed by the equation

$$\psi_{ea}(t) = L_e i_{ea}(t) + \psi_f cos(\theta_e(t)) \tag{5}$$

where L_e is the stator phase inductance: $L_e = L_{\sigma_e} + \frac{3M_{aa}}{2}$.

Extending Eq. (5) to the remaining stator phases gives

$$\psi_{eb}(t) = L_e i_{eb}(t) + \psi_f cos(\theta_e(t) - \frac{2\pi}{3}) \tag{6}$$

$$\psi_{ec}(t) = L_e i_{ec}(t) + \psi_f cos(\theta_e(t) + \frac{2\pi}{3}) \tag{7}$$

where

$\psi_{eb}(t)$ Total instantaneous flux in the stator phase "b",

$\psi_{ec}(t)$ Total instantaneous flux in the stator phase "c".

The voltage at the stator windings is

$$\begin{aligned} v_{ea}(t) &= R_e i_{ea}(t) + \frac{d\psi_{ea}(t)}{dt} \\ &= R_e i_{ea}(t) + L_e \frac{di_{ea}(t)}{dt} - \psi_f \omega_e(t) sin(\theta_e(t)) \end{aligned} \tag{8}$$

where

R_e Equivalent resistance of one stator phase,

$\omega_e(t)$ Angular speed of the electrical rotor.

Eq. (9) establishes the relationship between the angular speeds of the electrical and mechanical rotors:

$$\frac{d\theta_e(t)}{dt} = \omega_e(t) = p\omega_g(t) \tag{9}$$

where p is the number of pole pairs and $\omega_g(t)$ is the angular speed of the mechanical rotor.

Extending Eqs. (8) and (9) to the remaining phases and using the vectorial notation gives

$$\begin{bmatrix} v_{ea}(t) \\ v_{eb}(t) \\ v_{ec}(t) \end{bmatrix} = (R_e + L_e \frac{d}{dt}) \begin{bmatrix} i_{ea}(t) \\ i_{eb}(t) \\ i_{ec}(t) \end{bmatrix} - \psi_f \omega_e(t) \begin{bmatrix} sin(\theta_e(t)) \\ sin(\theta_e(t) - \frac{2\pi}{3}) \\ sin(\theta_e(t) + \frac{2\pi}{3}) \end{bmatrix} \tag{10}$$

The parameters R_e and L_e are required in Eq. (10). To obtain R_e, a high-precision multimeter is used. To take into account the relationship between the resistance and the temperature, Eq. (11) is used [16].

$$R_{T_i} = R_{T_r} \frac{235 + T_i}{235 + T_r} \tag{11}$$

Here,

R_{T_i} Resistance at the desired temperature [Ω],

R_{T_r} Resistance at room temperature [Ω],

T_r Room temperature [°C],

T_i Desired temperature [°C].

To obtain L_e, the formulation proposed in [17, 18, 19] is used. The PMSM model is shown in Fig. 1.

Figure 1

Figure 2

After obtaining the PMSM model, the effects of the inverter and the grid must be incorporated into the system model. For this purpose, a variable resistor R will be defined (see Fig. 2). This resistor R will control the power injected into the grid.

To consider the efficiency of the inverter, a study of the inverter losses ΔP_{inv} was conducted (see Fig. 3). Thus, the relationship between continuous current in the rectifier i_{dc} and the inverter losses ΔP_{inv} was obtained. Therefore, the grid power P_{grid} can be calculated as

$$P_{grid} = P_{dc} - \Delta P_{inv} = v_{dc} i_{dc} - 16.06\, e^{0.149\, i_{dc}} \tag{12}$$

where P_{dc} is the DC power of the rectifier and v_{dc} is the DC voltage of the rectifier.

Figure 3

The final system model will be used to analyse the SWT performance when certain parameters are modified, such as the rotation speed n, the capacitance value C and the variable resistor R (see Fig. 2). Therefore, the following values can be obtained:

- The grid power P_{grid} and the rectifier DC voltage v_{dc} by combining different values of R, C and n.
- The MPCC for different operating conditions.

3. MAXIMUM POWER POINT TRACKER (MPPT)

A SWT converts the kinetic energy of wind into electrical energy. A mechanical torque is produced when air passes through the turbine blades. This torque is used by the PMSM to produce three-phase power at a variable frequency. A back-to-back converter then transforms this AC power into AC power with fixed frequency.

The equation that relates the wind speed u_h with the mechanical power at the wind turbine rotor P_w is

$$P_w = \left(\frac{1}{2}\,\frac{\pi\, d^2}{4}\,\rho\, u_h^3\right) C_p(\lambda, \beta) \tag{13}$$

where

- C_p Power coefficient. The maximum value that can be achieved is 16/27, which is known as the Betz limit [20],
- P_w Mechanical power at the wind turbine rotor [W],
- u_h Wind speed [m/s],
- d Diameter of the swept area [m],
- ρ Air density [kg/m^3],
- β Pitch angle [°],
- λ Tip speed ratio.

Hence, the mechanical power obtained by the SWT is a function of u_h and of certain aerodynamic parameters. Eq. (13) depends on the tip speed ratio λ, and this parameter can be calculated with Eq. (14),

$$\lambda = \frac{\omega \frac{d}{2}}{u_h} = \frac{\frac{2\pi n}{60}\frac{d}{2}}{u_h} \tag{14}$$

where

- ω SWT angular speed [rad/s],
- n SWT rotation speed [rpm].

Alternatively, Eq. (13) can be expressed in terms of torque by

$$P_w = T_w \omega \tag{15}$$

where T_w is the SWT torque [Nm].

For each SWT, there is a single value of λ that provides the highest value of C_p and, according to Eq. (13), the highest mechanical power P_w. Thus, according to Eq. (14), each u_h has an optimum value of n that keeps λ constant. Therefore, the example in Fig. 4 shows the mechanical power P_w with respect to the SWT rotation speed n. The wider line indicates the maximum mechanical power at various wind speeds and is known as the Maximum Power Point Tracker (MPPT) [12].

With Eq. (15), the associated mechanical torque T_w at various wind speeds u_h can also be obtained, which is known as the Torque Point Tracker (TPT).

Figure 4

4. METHODOLOGY TO CALCULATE THE OPTIMAL CAPACITOR BANK AND MPCC

The flowchart to calculate the optimal capacitor bank and its associated MPCC is shown in Fig. 5. The steps of the methodology are as follows:

Step 1: Perform several tests on the SWT. At a minimum, a no-load test and a rated load test should be conducted.

Step 2: Define a system model. Adjust the model parameters by comparing the simulation results with those obtained in Step 1.

Figure 5

Step 3: Calculate the TPT to extract the maximum mechanical power. Given Eq. (13),

$$P_w = f(d, \rho, n, u_h, \beta) \Rightarrow \{d, \rho\, and\, \beta\, are\, constants\} \Rightarrow P_w = f(n, u_h) \quad (16)$$

In this way, the maximum mechanical power $P_{w_{max_i}}$ and its associated rotation speed n_i for each wind speed u_{h_i} can be obtained by deriving P_w with respect to n and setting the result to zero.

$$\left.\frac{dP_w}{dn}\right|_{u_{h_i}} = 0 \Rightarrow \left[P_{w_{max_i}}, n_i\right]_{u_{h_i}} \tag{17}$$

Using Eq. (15), the mechanical torque $T_{w,P_{w_{max_i}}}$ associated with each $P_{w_{max_i}}$ can be calculated. Thus,

$$T_{w,P_{w_{max_i}}}\Big|_{u_{h_i}}^{n_i} = \frac{P_{w_{max_i}}\Big|_{u_{h_i}}^{n_i}}{\omega_i} \tag{18}$$

Note that the TPT must remain unchanged for every value of the variable resistor R. Therefore, the TPT in 3D can be represented as a surface parallel to axis R.

Step 4: Calculate a capacitance range [C_1-C_2] that contains the optimal capacitor C. Using the Simulink model, perform a simulation that varies R and C for the rated speed of the SWT (see the example in Fig. 6). The initial ranges of R and C must be sufficiently wide to effectively analyse the SWT performance.

Figure 6

Looking at Fig. 6, it can be seen that by increasing the capacitance C (for a constant value of R) the power injected to the grid P_{grid} increases, up to reach a maximum capacitance value C_{max}, from which point P_{grid} decreases.

However, the value of C_{max} must be controlled because it could also increase the current i_r flowing into the PMSM windings and thereby cause

damage.

$$i_r = f(R, C, n) \Rightarrow \{n = n_{rated}\} \tag{19}$$

Therefore, the winding wire diameter should be known to determine the maximum current $i_{r,max}$ that can flow through windings. Once the value of $i_{r,max}$ is known, the capacitance range [C_1-C_2] can be obtained by means of drawing a perpendicular surface to the axis i_r (see the example in Fig. 7 and Fig. 8).

$$i_r\Big|_{n_{rated}} = f(R, C) \Rightarrow [C_1 - C_2]\Big|_{n_{rated}}^{i_r \leq i_{r,max}} \tag{20}$$

Figure 7

Figure 8

Step 5: Obtain MPCCs for several values of C_j: ($C_1 \leq C_j \leq C_2$). The greater the number of values of C_j that are tested, the more accurate the results will be. For each value of C_j, the following steps must be performed:

- Step 5.1: Use the system model to determine the operating surface $T_w(R, n)$ of the SWT.

$$T_w = f(R, C, n) \Rightarrow \{C = C_j\} \Rightarrow T_w\Big|_{C_j} = f(R, n) \tag{21}$$

  Then, obtain the intersection of that surface with the TPT (see the example in Fig. 9). Thus, the relationship $R(n)\big|_{P_{w_{max}}}^{C=C_j}$ for maximum mechanical power extraction from the wind is obtained (see Fig. 10).

Figure 9

Figure 10

- Step 5.2: Project the optimal relationship $R(n)\big|_{P_{wmax}}^{C=C_j}$ perpendicular to the R-n plane (see the example in Fig. 11).

- Step 5.3: Use the model to determine the SWT operating surfaces $P_{grid}(R,n)$ (see the example in Fig. 11) and $v_{dc}(R,n)$ (see the example in Fig. 12).

$$P_{grid} = f(R,C,n) \Rightarrow \{C = C_j\} \Rightarrow P_{grid}\Big|_{C_j} = f(R,n) \tag{22}$$

$$v_{dc} = f(R,C,n) \Rightarrow \{C = C_j\} \Rightarrow v_{dc}\Big|_{C_j} = f(R,n) \tag{23}$$

  Then, obtain the intersection of those SWT surfaces with the surface obtained in Step 5.2. In this way, the optimal relationships $P_{grid}(n)\big|_{P_{wmax}}^{C=C_j}$ and $v_{dc}(n)\big|_{P_{wmax}}^{C=C_j}$ can be determined.

- Step 5.4: Finally, the optimal relationship $P_{grid}(v_{dc})\big|_{P_{wmax}}^{C=C_j}$, also known as the MPCC, can be determined easily with the values of $P_{grid}(n)\big|_{P_{wmax}}^{C=C_j}$ and $v_{dc}(n)\big|_{P_{wmax}}^{C=C_j}$ (see the example in Fig. 13).

Figure 11

Figure 12

Figure 13

The additional MPCCs can be obtained by repeating steps 5.1 to 5.4 for each value of C_j.

Step 6: Analyse the results and perform an economic study. To perform the analysis, the well-known Weibull Distribution (WD) can be used [12, 15].

This distribution is defined as

$$W(u_h) = \frac{K}{u_h}\left(\frac{u_h}{u_m}\right)^K e^{-\left(\frac{u_h}{u_m}\right)^K} \tag{24}$$

where K is the shape parameter of the WD, and u_m is the average wind speed.

The National Renewable Energy Laboratory (NREL) defines seven different Wind Classes (WCs). Each WC is a function of the average wind speed u_m and the height at which the SWT is located (10 or 50 m) with respect to the ground [21]. These WCs are shown in Table 1.

The Weibull Distributions, Eq. (24), for a value of K=1.9 and for the average wind speeds listed in Table 1 (assuming a height of 10 m) are shown in Fig. 14.

Table 1

Figure 14

To compare the results obtained with different values of C_j, four parameters will be used: $E(u_{h_i})$, E_{tot}, $\Delta\eta\Big|_{C_j}$ and $\Delta\$\Big|_{C_j}$.

- $E(u_{h_i})$ is the annual grid energy for each wind speed u_{h_i} and is defined as

$$E(u_{h_i}) = 8760\left[\frac{hours}{year}\right] W(u_{h_i}) P_{grid}(u_{h_i}) \tag{25}$$

  where $P_{grid}(u_{h_i})$ is the SWT grid power for each wind speed u_{h_i}.

- E_{tot} is the annual total energy that can be produced by the SWT. It is obtained from the following equation:

$$E_{tot} = \sum_{i=0}^{n} E(u_{h_i}) \tag{26}$$

- $\Delta\eta\Big|_{C_j}$ represents the annual total energy increment injected into the grid for different capacitor banks (C=C_j) compared to the case without a capacitor bank (C=0).

$$\Delta\eta\Big|_{C_j} = \frac{E_{tot,C=C_j} - E_{tot,C=0}}{E_{tot,C=0}} \tag{27}$$

- $\Delta\$\Big|_{C_j}$ represents the annual financial benefit obtained by using different capacitor banks (C=C_j) compared to the case without a capacitor bank (C=0). In the calculations, an energy cost of 0.2484 US$/kWh is assumed (including electricity taxes).

$$\Delta\$\Big|_{C_j} = \left(E_{tot,C=C_j} - E_{tot,C=0}\right) 0.2484 \left[\frac{US\$}{kWh}\right] \tag{28}$$

5. SET-UP FACILITY

The architecture of the set-up facility is depicted in Fig. 15. The main elements are as follows:

Figure 15

- DC motor to simulate wind effects (5 H.P. and 200 V),
- PMSM of the SWT,
- Rectifier (AC ⇒ DC),
- Inverter (DC ⇒ AC),
- Six-channel wattmeter,

- Power quality analyser,
- Torque and speed sensors,
- Multimeter to measure the PMSM phase resistance,
- Temperature sensors in windings,
- PC to control the wattmeter, the temperature sensors and the inverter.

Fig. 16 shows the connection of the different devices.

Figure 16

6. RESULTS

This methodology and the set-up facility were used to optimise a commercial SWT whose rated parameters are as follows:

- Number of blades: 3,
- Power coefficient: 0.36,
- Diameter: 4.2 m,
- Rated speed of the wind: 11 m/s,
- Rated speed: 250 rpm,
- PMSM rated power: 3500 W,
- Pole pairs: 10.

The results obtained were as follows:

Steps 1 and 2: Various tests were performed, and the results were compared with the simulated results. Fig. 17 represents the continuous voltage v_{dc} and the PMSM phase voltage v_r versus the rotation speed n. The simulated results show a high degree of agreement with the real values.

Figure 17

Step 3: The TPT was calculated. Table 2 shows the results obtained when the methodology was applied. These results are for the case when no capacitor bank was connected (C=0).

Table 2

Step 4: The capacitance range was obtained. If the winding wire diameter is 0.8 mm, the maximum allowed current is approximately 11 A. Thus, the capacitance C is calculated to be between C_1=0 and C_2=25 μF, for every value of R. The capacitances tested were 0, 4, 6, 8, 10, 12, 14, 16, 20, and 24 μF.

Step 5: MPCCs for several values of C were calculated. The simulated results without the use of capacitor banks (C=0) are shown in Table 2.

The remaining MPCCs were determined by repeating this step for the different capacitances. These curves are shown in Fig. 18.

Table 3 presents the values of P_{grid} that were obtained for different wind speeds u_{h_i} for each capacitance C_j. This table also shows the capacitance value that produces the highest P_{grid} for each wind speed u_{h_i} (highlighted values).

Figure 18

Table 3

Step 6: An analysis of the results and an economic study were performed. Using the WD Eq. (24) and assuming WC=2 (height 10 m) lead to the results shown in Table 4. This table shows $E(u_{h_i})$, E_{tot}, $\Delta\eta\Big|_{C_j}$ and $\Delta\$\Big|_{C_j}$.

As Table 4 shows, the highest benefit ($41.51 USD) is produced by using a capacitance of 12 μF (4529 kWh). Given that capacitors cost approximately $14 USD, the total costs are covered in the first year. Thus, from the second year on, the capacitor bank would begin to make a profit.

Table 4

The analysis of the system financial benefits for the remaining WCs (height=10 m) led to the results shown in Table 5.

Table 5

Table 5 shows that the investment can be recovered during the first year of use for WC values equal to or greater than 3. The value of the optimal capacitance varies for each WC. Hence, it is necessary to know the location of the SWT to choose the capacitor bank that yields the maximum efficiency.

Table 6 shows the efficiency increase produced when using different capacitor banks and WCs. For WC=2 and height=10 m, the efficiency increase was 3.83%.

Table 6

Once the simulated results were obtained, an experiment was conducted to verify them. The test consisted of connecting a capacitor bank of 12 μF (delta connection) to the SWT. The simulated and experimental results are shown in Fig. 19.

Figure 19

7. CONCLUSIONS

The increasing development of small-wind energy systems has made it necessary to study new methods to improve the efficiency of this technology. This paper presents a methodology to increase the SWT efficiency by connecting a capacitor bank. This methodology involves the use of a Simulink model to simulate the system.

The results obtained with the Simulink model are suitable because they show a high degree of agreement with the performance of the real machine. As an example, the efficiency increases predicted by the simulations were the same as those obtained in the real tests. Given the accuracy of the Simulink model, all modifications can be extrapolated to the SWT.

It has been shown that connecting different capacitor banks to the system modifies the SWT performance and the MPCC. The power obtained from the SWT increases as a result of connecting capacitor banks and is only limited by the maximum current that can flow through the PMSM windings. To connect the optimal capacitor bank, the precise location of the SWT and the associated average wind speed must be known. In this study, we found that connecting a capacitor bank of 12 μF increases the SWT efficiency by

3.83%. Thus, in the PMSM design, an added shunt capacitance could be a new parameter to bear in mind.

The methodology described in this paper could be used by electrical machine manufacturers to reduce the PMSM size. If the 3.5 kW PMSM is redesigned using a capacitor bank, this new electrical machine will contain less copper (the capacitor bank decreases the current that flows through the PMSM), a smaller magnet size (due to magnetising effect of the capacitors) and fewer magnetic plates to obtain the same electrical power P_{grid}. If these modifications are included in the SWT design, the manufacturing costs would decrease substantially, especially in the case of higher WCs.

Acknowledgment

The authors are grateful for the support from the Spanish Government under the project ENE2007-68032-C04-04, SODERCAN, ITEC and Sonkyo Energy.

References

[1] Succar S, Denkenberger DC, Williams RH. Optimization of specific rating for wind turbine arrays coupled to compressed air energy storage. Appl. Energy 2012; doi: 10.1016/j.apenergy.2011.12.028.

[2] Eriksson S, Bernhoff H. Loss evaluation and design optimisation for direct driven permanent magnet synchronous generators for wind power. Appl. Energy 2011;88:265–71.

[3] De Paor AM. Aerodynamic design of optimum wind turbines. Appl. Energy 1982;12:221–8.

[4] Power MH. A simulation model for wind turbines. Appl. Energy 1980;6:395–9.

[5] Melcio R, Mendes V, Catalo J. Transient analysis of variable-speed wind turbines at wind speed disturbances and a pitch control malfunction. Appl. Energy 2011;88:1322–30.

[6] Arifujjaman M, Iqbal M, Quaicoe J. Reliability analysis of grid connected small wind turbine power electronics. Appl. Energy 2009;86:1617–23.

[7] Milivojevic N, Stamenkovic I, Schofield N, Emadi A. Electrical machines and power electronic drives for wind turbine applications. 34th Annual Conference of IEEE Industrial Electronics. IECON 2008 2008;2326–31.

[8] Yingtao M, Xudong S, Jianyun C. Three-phase PFC rectifier with sensorless control for PMSG wind generation system. 2011 International Conference on Electrical Machines and Systems (ICEMS) 2011;1:1–4.

[9] Sahoo SK, Jariwala HR. A new power factor correction technique using PFC boost converter. 2012 11th International Conference on Environment and Electrical Engineering (EEEIC) 2012;1:819–23.

[10] Matlab-Simulink. User's manual, (2008).

[11] Kesraoui M, Korichi N, Belkadi A. Maximum power point tracker of wind energy conversion system. Renew. Energy 2011;36:2655–62.

[12] Milivojevic N, Stamenkovic I, Schofield N. Power and energy analysis

of commercial small wind turbine systems. International Conference on Industrial Technology (ICIT) 2010;1739–44.

[13] Fuchs E, Vandenput A, Holl J, White J. Design analysis of capacitor-start, capacitor-run single-phase induction motors. IEEE Transactions on Energy Conver. 1990;5:327–36.

[14] Idjdarene K, Rekioua D, Rekioua T, Tounzi A. Vector control of autonomous induction generator taking saturation effect into account. Energy Convers. and Manage. 2008;49:2609–17.

[15] Sathyajith M. Wind energy. Fundamentals, resource analysis and economics 2006;1–167.

[16] EN 60034-2-1, Rotating electrical machines - Part 2-1: Standard methods for determining losses and efficiency from tests (excluding machines for traction vehicles) 2007, p. 1–80.

[17] IEEE Std 1110, Guide for Synchronous Generator Modelling Practices and Applications in Power System Stability Analyses 2002, p. 1–72.

[18] Mulukutla S. Synchronous Machines. Their Theory, Stability and Excitation Systems. In: Gordon and Breach, Science Publishers, Inc 1979, p. 97–170.

[19] IEEE Std 115, Guide: Test Procedures for Synchronous Machines Part I- Acceptance and Performance Testing Part II- Test Procedures and Parameter Determination for Dynamic Analysis 2010, p. 1–219.

[20] Van Kuik GA. The lanchester betz joukowsky limit. Wind Energy 2007;10:289–91.

[21] Elliot DL, Holladay CG, Barchet WR, Foote HP, Sandusky WF. Wind energy resource atlas of the United States 1986.

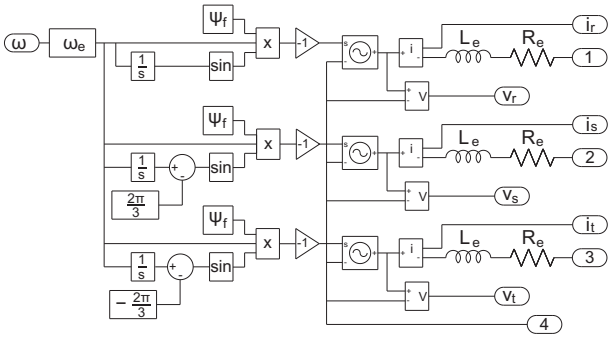

Figure 1:

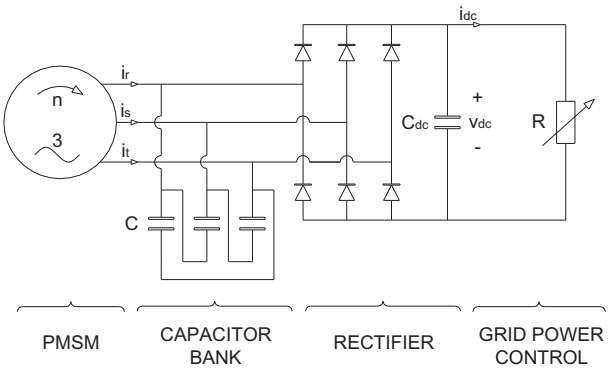
idc
ir
is
it
n
3
C
Cdc
+
vdc
-
R
PMSM
CAPACITOR BANK
RECTIFIER
GRID POWER CONTROL

Figure 2:

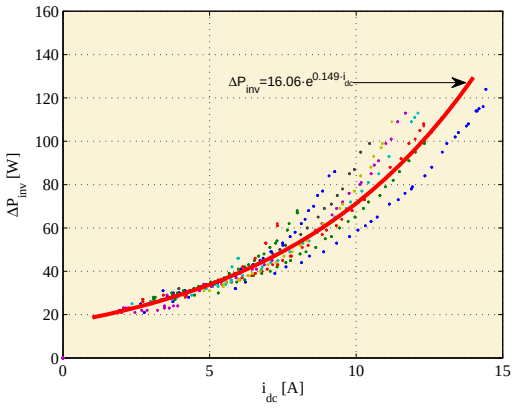
160
140
120
100
80
60
40
20
0
0
5
10
15
ΔP_inv=16.06·e^0.149·i_dc
ΔP_inv [W]
i_dc [A]

Figure 3:

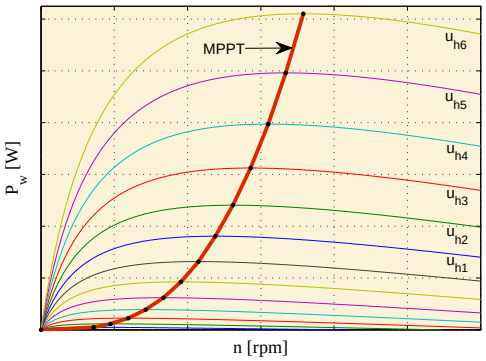

Figure 4:

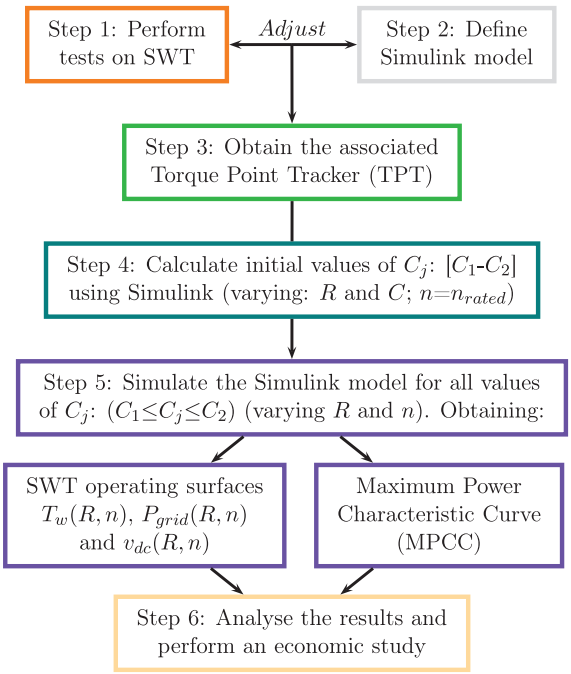
Step 1: Perform tests on SWT
Adjust
Step 2: Define Simulink model
Step 3: Obtain the associated Torque Point Tracker (TPT)
Step 4: Calculate initial values of C_j: [C_1-C_2] using Simulink (varying: R and C; n=n_{rated})
Step 5: Simulate the Simulink model for all values of C_j: ($C_1 \leq C_j \leq C_2$) (varying R and n). Obtaining:
SWT operating surfaces $T_w(R,n)$, $P_{grid}(R,n)$ and $v_{dc}(R,n)$
Maximum Power Characteristic Curve (MPCC)
Step 6: Analyse the results and perform an economic study

Figure 5:

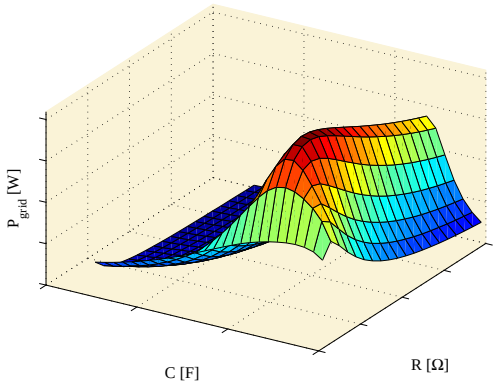

Figure 6:

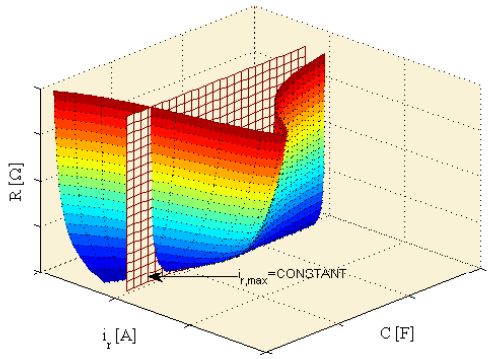

Figure 7:

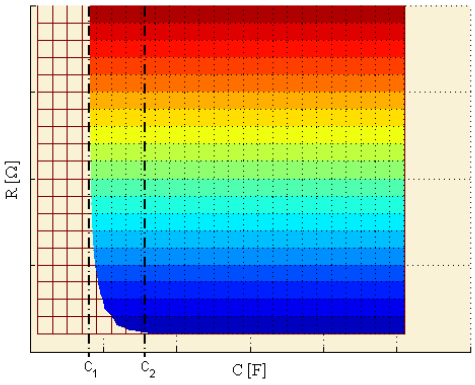

Figure 8:

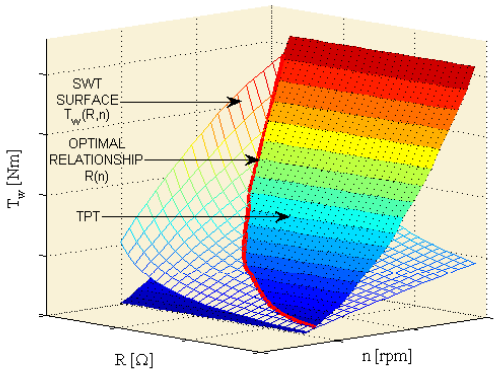

Figure 9:

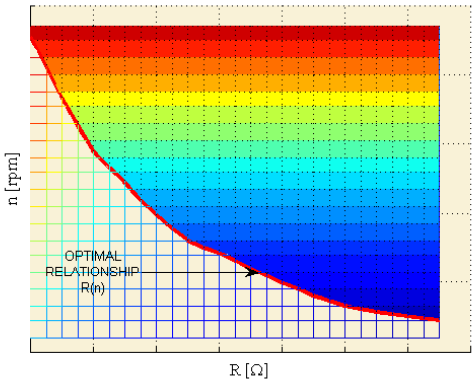

Figure 10:

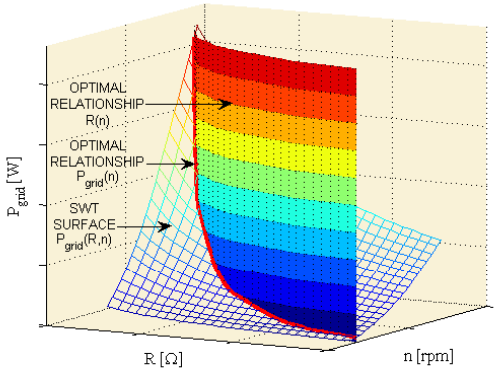
OPTIMAL
RELATIONSHIP
R(n)
OPTIMAL
RELATIONSHIP
P grid(n)
SWT
SURFACE
P grid(R,n)
P grid [W]
R [Ω]
n [rpm]

Figure 11:

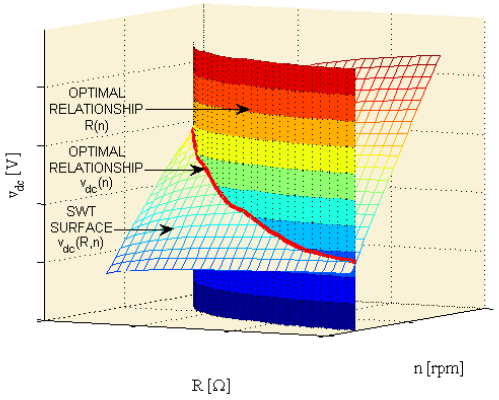
OPTIMAL
RELATIONSHIP
R(n)
OPTIMAL
RELATIONSHIP
$v_{dc}(n)$
SWT
SURFACE
$v_{dc}(R,n)$
v_{dc} [V]
R [Ω]
n [rpm]

Figure 12:

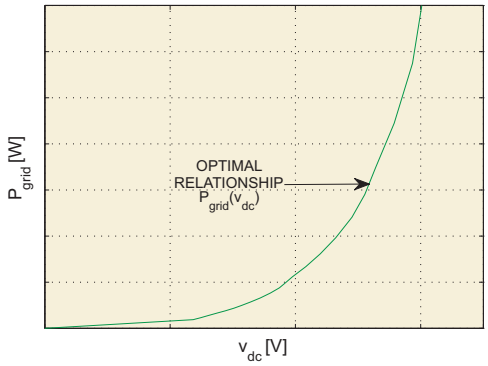

Figure 13:

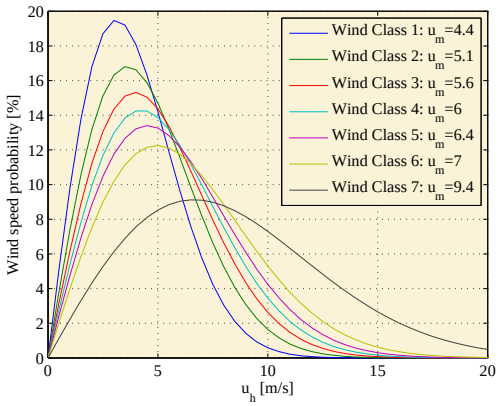
Wind speed probability [%]
u_h [m/s]
Wind Class 1: u_m=4.4
Wind Class 2: u_m=5.1
Wind Class 3: u_m=5.6
Wind Class 4: u_m=6
Wind Class 5: u_m=6.4
Wind Class 6: u_m=7
Wind Class 7: u_m=9.4

Figure 14:

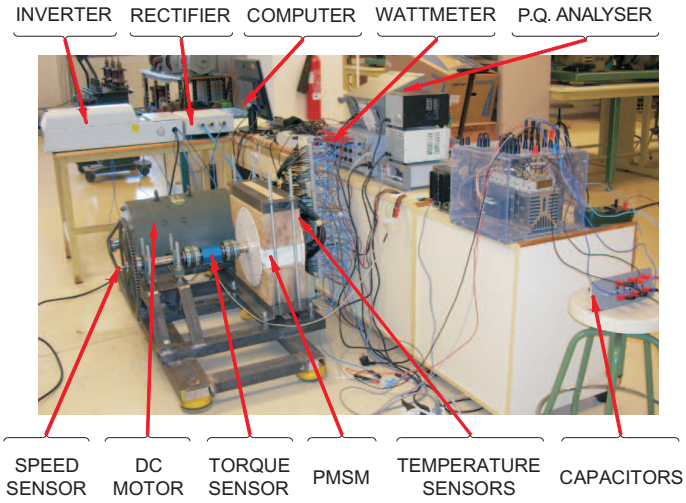
INVERTER
RECTIFIER
COMPUTER
WATTMETER
P.Q. ANALYSER
SPEED SENSOR
DC MOTOR
TORQUE SENSOR
PMSM
TEMPERATURE SENSORS
CAPACITORS

Figure 15:

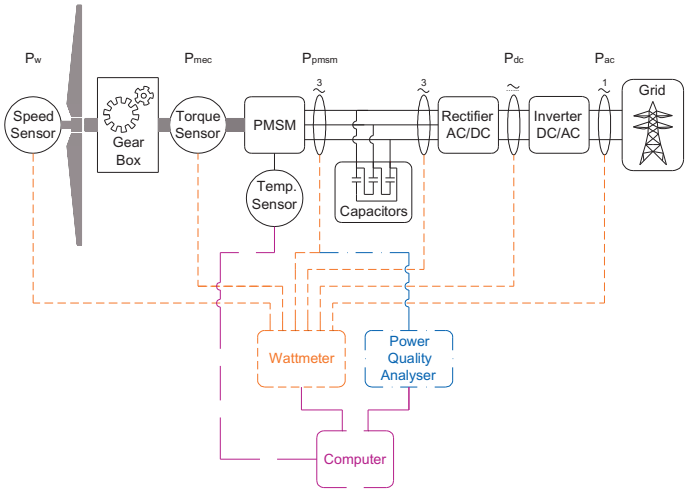
Pw
Pmec
Ppmsm
Pdc
Pac
Speed Sensor
Gear Box
Torque Sensor
PMSM
Temp. Sensor
Capacitors
Rectifier AC/DC
Inverter DC/AC
Grid
Wattmeter
Power Quality Analyser
Computer

Figure 16:

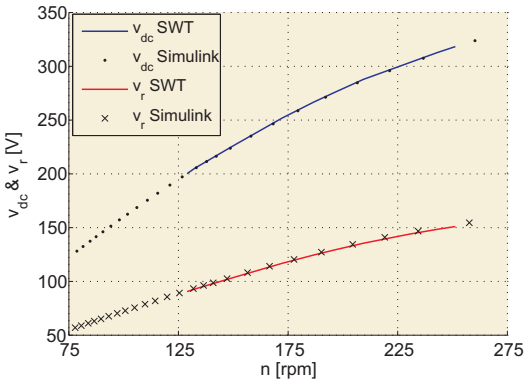
v_dc SWT
v_dc Simulink
v_r SWT
v_r Simulink
v_dc & v_r [V]
n [rpm]
350
300
250
200
150
100
50
75
125
175
225
275

Figure 17:

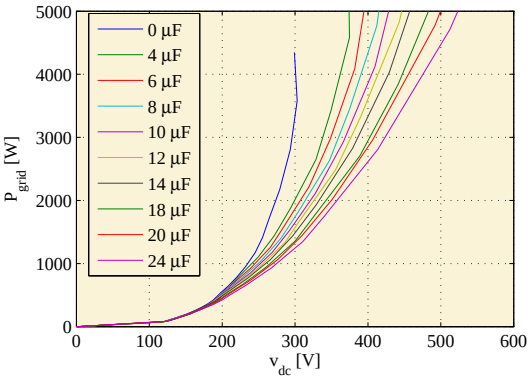
5000
4000
3000
2000
1000
0
0
100
200
300
400
500
600
P grid [W]
v dc [V]
0 µF
4 µF
6 µF
8 µF
10 µF
12 µF
14 µF
18 µF
20 µF
24 µF

Figure 18:

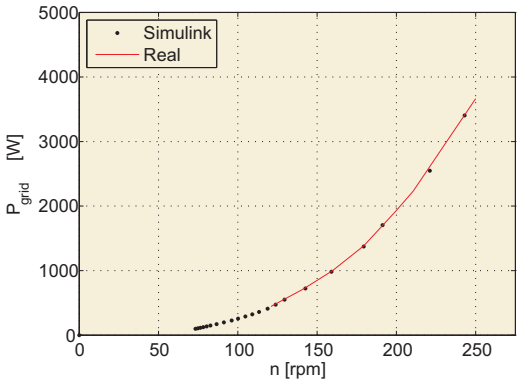
Simulink
Real
5000
4000
3000
2000
1000
0
P grid [W]
0
50
100
150
200
250
n [rpm]

Figure 19:

β	Pitch angle [°].
ΔP_{inv}	Inverter losses [W].
$\Delta\eta$	Increment of E_{tot} using different capacitor banks [%].
$\Delta\$$	Annual benefit [\$].
λ	Tip speed ratio.
C	Capacitance of the capacitor banks [F].
C_{dc}	DC bus capacitor [F].
C_p	Power coefficient.
d	Diameter of turbine blades [m].
E_{tot}	Annual total energy extracted from the SWT [kWh].
$E\,(u_h)$	Annual grid energy for each wind speed [kWh].
i_{dc}	DC Rectifier current [A].
i_r, i_s, i_t	Phase RMS current of the PMSM [A].
n	SWT rotation speed [rpm].
P_{dc}	Rectifier DC power [W].
P_{grid}	Grid power [W].
P_w	Mechanical power at the wind turbine rotor [W].
R	Variable resistor to simulate inverter and grid effects [Ω].
T_w	Torque in SWT shaft [Nm].
u_h	Wind speed [m/s].
v_{dc}	DC Rectifier voltage [V].
v_r, v_s, v_t	Phase RMS voltage of the PMSM [V].
$W(u_h)$	Weibull distribution.

Figure 20: Glossary

Table 1:

Wind Class	u_m (10 m)	u_m (50 m)
1	0 - 4.4	0 - 5.6
2	4.4 - 5.1	5.6 - 6.4
3	5.1 - 5.6	6.4 - 7
4	5.6 - 6	7 - 7.5
5	6 - 6.4	7.5 - 8
6	6.4 - 7	8 - 8.8
7	7 - 9.4	8.8 - 11.9

Table 2:

Step 3				Step 5	
u_{h_i}	n	T_w	R	P_{grid}	v_{dc}
11.9	276.9	194.5	20	4346.1	299.2
10.1	233.2	138.8	30	2804.7	293.5
9.2	213.3	115.4	35	2170.3	278.8
8.4	194.9	97.7	40	1702.6	264.1
7.4	172.2	74.6	50	1171.0	245.1
6.0	139.2	50.2	65	644.0	208.3
5.0	116.0	33.9	85	361.2	180.1
4.1	95.0	23.3	105	197.2	150.9
3.1	72.7	13.0	150	75.1	118.5

Table 3:

$u_{h_i}[m/s]$	$P_{grid}[W]$					
	$0\mu F$	$6\mu F$	$8\mu F$	$10\mu F$	$12\mu F$	$14\mu F$
5.0	360	361	360	358	358	359
6.0	643	645	651	648	647	650
7.0	995	1010	1008	1014	1010	1007
8.0	1464	1503	1496	1504	1500	1492
9.0	2054	2122	2141	2120	2143	2135
10.0	2763	2888	2877	2888	2900	2870
11.0	3572	3784	3817	3807	3846	3804
12.0	4401	4834	4822	4895	4855	4922

Table 4:

u_{h_i}	$E(u_{h_i})$ [kWh]					
	$0\mu F$	$6\mu F$	$8\mu F$	$10\mu F$	$12\mu F$	$14\mu F$
5	441.1	442.5	441.0	438.9	438.9	440.2
6	622.5	624.6	629.3	627.6	626.3	629.0
7	696.4	707.0	705.6	709.2	706.9	704.7
8	682.1	699.5	697.0	700.1	698.5	695.1
9	589.7	609.1	614.6	608.6	614.9	612.8
10	454.4	474.8	473.0	474.8	476.7	471.8
11	313.4	332.1	335.0	334.1	337.4	333.8
12	174.2	211.5	211.0	214.1	212.4	215.3
E_{tot}	4362	4517	4523	4526	4529	4522
$\Delta\eta \Rightarrow$		3.56	3.68	3.77	3.83	3.65
$\Delta\$ \Rightarrow$		38.65	39.92	40.82	41.51	39.56

Table 5:

WC	$\Delta\$$ (Height = 10 m)				
	$6\mu F$	$8\mu F$	$10\mu F$	$12\mu F$	$14\mu F$
1	15.4	15.9	16.1	15.8	15.1
2	38.6	39.9	40.9	41.5	39.7
3	66.2	67.1	69.3	70.4	68.3
4	94.0	94.3	98.2	99.3	97.5
5	124.2	125.5	131.3	132.2	131.1
6	175.1	176.4	185.6	185.8	186.3
7	356.8	357.3	380.2	375.4	385.5

Table 6:

WC	$\Delta\eta$ [%] (Height = 10 m)				
	$6\mu F$	$8\mu F$	$10\mu F$	$12\mu F$	$14\mu F$
1	2.21	2.25	2.25	2.26	2.13
2	3.62	3.68	3.77	3.83	3.67
3	4.76	4.83	4.99	5.06	4.92
4	5.67	5.74	5.97	6.03	5.93
5	6.54	6.61	6.91	6.95	6.90
6	7.73	7.79	8.19	8.20	8.22
7	10.96	10.97	11.68	11.53	11.84

Figure Captions

FIGURES

Figure 1: PMSM schematic generated using Matlab.

Figure 2: Wind power generation system.

Figure 3: DC current of the rectifier i_{dc} vs. inverter losses ΔP_{inv}.

Figure 4: Turbine rotation speed n vs. mechanical power P_w for different wind speeds u_h.

Figure 5: Flowchart of the methodology.

Figure 6: Grid power P_{grid} vs. resistance R and capacitance C for the rated speed n_{rated}.

Figure 7: Winding current i_r vs. resistance R and capacitance C.

Figure 8: Relationship R(C) not exceeding the restriction of $i_{r,max}$ for the rated speed of the SWT.

Figure 9: Intersection between the TPT and the operating surface $T_w(R,n)$ of the SWT.

Figure 10: Optimal relationship $R(n)|_{Pwmax}$.

Figure 11: Intersection between the optimal relationship R(n) and the operating surface $P_{grid}(R,n)$ of the SWT.

Figure 12: Intersection between the optimal relationship R(n) and the operating surface $v_{dc}(R,n)$ of the SWT.

Figure 13: Maximum Power Characteristic Curve (MPCC): Grid power P_{grid} vs. rectifier DC voltage v_{dc}.

Figure 14: Weibull distribution for different WCs at a height of 10 m.

Figure 15: System: PMSM + Rectifier + Inverter + Capacitor bank.

Figure 16: SWT block diagram.

Figure 17: Real and simulated results.

Figure 18: MPCCs obtained with different capacitor banks.

Figure 19: Simulated and experimental results (C=12µF).

Figure 20: Glossary.

TABLES